AEDC-TDR-62-122

COMPENSATION OF DYNAMIC STING EFFECTS IN HOTSHOT FORCE MEASUREMENTS

By

E. E. Edenfield and R. L. Ledford

von Kármán Gas Dynamics Facility

ARO, Inc.

a subsidiary of Sverdrup and Parcel, Inc.

June 1962

ARO Project No. 366983

AF - AEDC
Arnold AFS Tenn

FOREWORD

The efforts of D. S. Bynum and W. E. Smotherman of ARO, Inc., are largely responsible for the development of the compensating system reported herein. Acknowledgment of similar work (Ref. 1) performed at the Cornell Aeronautical Laboratory is also made.

ABSTRACT

A system which can substantially reduce the detrimental effects of sting vibrations on force measurements made in the von Kármán Gas Dynamics Facility's Hotshot wind tunnels has been developed and proved effective. A description of this system and its theory of operation are presented along with the results of evaluation tests.

CONTENTS

ILLUSTRATIONS

NOMENCLATURE

A	Area of the model base, 7.06 in.^{2}
C_A	Axial-force coefficient, F_A/qA
C_N	Normal-force coefficient, F_N/qA
C_{N_A}	Aft gage normal-force coefficient, F_{N_A}/qA
C_{N_F}	Forward gage normal-force coefficient, F_{N_F}/qA
C_m	Pitching moment coefficient, M_y/qAd
c	Coefficient of viscous damping, lb-sec/ft
c_c	Critical damping coefficient, lb-sec/ft
d	Model base diameter, 3 in.
F_A	Axial force, lb
F_N	Normal force, lb
F_{N_A}	Aft gage normal force, lb
F_{N_F}	Forward gage normal force, lb
f	Frequency, cps
f_n	Natural frequency, cps
K	Spring rate, lb/in.
M	Free-stream Mach number
M_y	Pitching moment about a reference point 5.51 in. aft of nose, in.-lb
p_b	Model base pressure, psi
p_o'	Total pressure behind a normal shock at free-stream conditions, psi
Re	Free-stream Reynolds number based on the model length
t	Time, milliseconds
α	Angle of attack, deg
δ	Damping ratio, c/c_c

1.0 INTRODUCTION

Force measurements in the Hotshot tunnels are made with internal strain-gage balances. During the useful tunnel test time (5-80 msec), the model support system vibrates as a result of the shock load it receives during flow initiation. These vibrations cause the model-balance system to act as an accelerometer with the result that oscillations appear on the force data traces. Oscillations are also produced on the data traces by vibrations of the model itself. The combination of these oscillations prevents taking instantaneous data points unless a mean curve can be drawn through the data traces. This can generally be accomplished if the magnitude of the oscillation is not too great and the period is small compared to the run time. The foregoing requirements can be fulfilled in most cases with careful design and construction of model, balance, and sting. However, a system is desirable which would not place such stringent requirements on the model, balance, and sting, and which would reduce the detrimental effects of these vibrations on the data traces.

The design and development of a system which employs accelerometers to sense sting vibration and analog circuitry to cancel its effect on the force data has been completed. This system improves the quality of the data in two ways: 1) it reduces the effects of sting vibrations, and 2) it permits the use of heavier (and therefore stiffer) models which vibrate at frequencies which will not appear on the recording system employed. Both laboratory and tunnel tests have shown that the system operates satisfactorily.

This report gives the theory of operation of the sting-vibration-compensation system and briefly describes the system and evaluation tests which have been conducted on the system. This system was developed at the von Kármán Gas Dynamics Facility (VKF) of the Arnold Engineering Development Center (AEDC), Air Force Systems Command (AFSC), USAF, Arnold Air Force Station, Tennessee.

2.0 THEORY OF OPERATION OF STING-VIBRATION-COMPENSATION SYSTEM

The model-balance-sting systems of the Hotshot tunnels may be represented schematically as shown in Fig. 1a. When a load is applied, the electrical signal produced by a strain-gage balance is directly proportional to the strain produced in K_B, which is the member upon which the strain gages are located.

Manuscript released by authors May 1962.

It can be seen that when the model support (sting) system vibrates, the model acts as an accelerometer mass and a force is produced on K_B. This force is proportional to the product of the mass of the model and the acceleration of the sting and has a frequency which is the same as that of the support system. The natural frequency of the Hotshot model support systems ranges from 30 to 100 cycles per second. The galvanometers which are employed for recording Hotshot force data have a natural frequency of 200 cycles per second. Therefore, vibration of the model support system during a tunnel run produces an oscillation at the sting frequency which is superimposed on the force data trace. With a relatively short run time ($\approx$ 5 msec) it becomes extremely difficult or even impossible to distinguish the aerodynamic load signal from the signal produced by the support system vibration.

If one adds another mass, supported by a spring K_A, which is attached to the support system at a position near K_B, this mass will also be subjected to the acceleration forces produced by the sting vibration. This mass and spring, which constitute an accelerometer, may be located inside the model so that they are not subjected to any aerodynamic forces. This combined system is shown in Fig. 1b.

The electrical signals produced by the strain in K_B and K_A will be unequal because of the differences in their respective masses, spring constants, etc. However, each of the signals may be amplified so that their oscillatory components are equal. After amplification, the signals may be introduced into a summing network which algebraically adds them. By properly phasing the signals (180 deg out of phase) and maintaining their oscillatory components at equal amplitudes, the sum of the oscillations may be made equal to zero. Therefore, any vibration of the model support system produces two oscillatory signals which cancel each other.

Proper phasing of the signals can be achieved easily if there is negligible phase shift between the forcing function and the deflections of the model and accelerometer masses. This may be accomplished by making the natural frequencies of the balance (with model attached) and accelerometers high in comparison to the sting natural frequency. Figure 2 is a graph of the phase angle between a forcing function and the deflection it produces, plotted for different values of damping. The value of damping in the balance and accelerometers is near zero, and the natural frequency of the model-balance is approximately 1000 cps, while that of the accelerometers is approximately 850 cps. From the graph it may be seen that for these values, with sting frequencies (forcing function) of 30 to 100 cps, there is no significant shift. With no phase shift, the signals from the balance and the

accelerometer must be in phase. By reversing the signal leads from the accelerometer, the signals are made 180 deg out of phase and cancellation may be achieved.

In a three-component balance, an accelerometer may be located near each load cell to sense the vibration at that point and with its associated circuitry, may effectively cancel the effects of sting vibrations on the data traces.

Figure 3b shows the theoretical signal produced by the load cells of a balance when subjected to a step force input (see Fig. 3a). In Fig. 3c the signal produced by the accelerometer is shown. It can be seen that reversing the polarity of the accelerometer signal and adding it to the load cell signal would produce the sum shown in Fig. 3d.

3.0 SYSTEM DESCRIPTION

The sting-vibration-compensation system is made up of four basic components: the force balance and its associated accelerometers, a carrier-amplifier system, summing networks, and a recording oscillograph. The system is shown in block form in Fig. 4.

The force balances which have been employed to data have been three-component, internal, strain-gage balances. The three components of force measured by these balances are axial, aft normal, and forward normal. Typical load ranges are: normal - 15 lb, axial - 5 lb.

The accelerometers which are used to sense the sting vibrations are composed of seismic masses mounted on cantilever beams. These beams are instrumented with electrical, bonded wire, strain gages which sense the beams' deflections. The natural frequency of accelerometers which have been built to date is typically 850 cycles per second. Figure 5 shows the location of the accelerometers in the balance; each accelerometer is placed as near as is physically possible to the load cell for which it provides compensation.

The summing networks employed with this system were designed by the VKF Instrumentation Branch; these networks have the following functions: 1) algebraically sum the signals from the balance load cells and their associated accelerometers, and 2) provide a means for monitoring the compensated data as well as the uncompensated data. A

schematic diagram of a summing circuit is shown in Fig. 6. This circuit was designed to supplement the filtering action of the recording galvanometers so that accelerometer vibrations would not appear on the data traces. A typical frequency response curve for the circuit is shown in Fig. 7.

The circuit is designed to properly match the output impedance of the carrier-amplifier system from which it is fed and to provide proper damping for the galvanometers. The function of the potentiometer R_1 (Fig. 6) is to allow the sensitivities of the compensated and uncompensated data channels for any component to be made equal. This is accomplished by applying a calibrate voltage at the force input of the network and adjusting R_1 until each galvanometer (compensated and uncompensated) for that channel deflects an equal amount; no accelerometer input is applied while making this adjustment. One summing network is required for each component of force; three units were employed for these tests.

To calibrate the sting-vibration-compensation system, it is necessary to produce vibration in the model support system while the balance, model, and sting are located in their test positions. With the carrier-amplifier system force-channel gain controls set at the value to be used for the test run, the accelerometer channel gain controls are adjusted to the positions which produce a minimum deflection of the galvanometers when the model support system is vibrated.

To produce vibration of the model support system, a shaker motor is attached to the sting near the base of the balance. Then, the frequency of the shaker is adjusted until sufficient vibration is present to enable the compensating system to be adjusted.

4.0 EVALUATION TESTS

4.1 LABORATORY TESTS

To evaluate the performance of the sting-vibration-compensation system, it was first subjected to a series of laboratory tests. These tests consisted of mounting a balance on a sting which was in turn mounted on a work bench; then, both step functions and oscillatory inputs were applied to the sting, and the compensated and uncompensated force outputs were observed for each type input. Several model masses were simulated in these tests. All of these tests indicated satisfactory performance of the system; i. e., compensation of the vibratory effects was attained.

4.2 WIND TUNNEL TESTS

Nineteen test runs were made in tunnel Hotshot 1 to obtain performance data under actual operating conditions. The support system employed in these tests was the conventional Hotshot 1 sting configuration. The force balance used was a three-component (axial, aft normal, forward normal) type. The balance was, of course, accelerometer instrumented.

The model configuration employed for all the tunnel tests was a 9-deg half-angle cone, shown in Fig. 8. The weight of the model was originally 52 grams; however, weights were added to the model at various times throughout the tests so that the acceleration effect, which was produced by the sting vibration, would be more pronounced. These weights were added at a point midway between the model's mounting pads. Model weights of 52, 100, 144, and 237 grams were tested. The compensation system was calibrated before each tunnel test run.

Test results are presented in Figs. 9 to 18. Typical oscillograph records are given in Figs. 9 to 11. In Figs. 12 to 14 the zeros of the compensated data have been shifted so that a direct comparison of the compensated and uncompensated data may be made. Oscillations at several different frequencies are present on the traces. The uncompensated normal-force channels show about one cycle of a 30 to 50 cps vibration at the sting fundamental frequency; the uncompensated axial-force channel shows several cycles of a 100-cps vibration which is the approximate frequency of the Hotshot 1 support system, and a 200-cps vibration caused by the model is present on both compensated and uncompensated normal-force channels. Typically the compensated trace is a reasonable fairing of the sting and support vibrations.

It is clear from Figs. 12 to 14 that as the model mass increases the amplitude of the uncompensated vibration increases. The compensation system performed as well with the heavy models as with the lightest one. However, the addition of weight to the model resulted in an increase in the magnitude of the oscillations caused by vibration of the model itself. Since model vibrations were not compensated by the sting-vibration-compensation system, rigid models are still a requirement.

Time variation of individual measurements with and without compensation are shown in Figs. 15 to 17 expressed as force coefficients. Large timewise variations in data which were taken without compensation were eliminated when compensation was used, even in the case of the heaviest model tested. The effect of increasing model weight nearly

fivefold was practically negligible with compensation. Without compensation, accurate interpretation of results obtained with the heavier models would be impossible.

The compensated data for all the models are compared with modified Newtonian theory in Fig. 18. The aerodynamic data obtained were the same regardless of model mass and compared favorably with the modified Newtonian theory. The axial-force data at $\alpha = 0$ are in agreement with data obtained previously in tunnel Hotshot 2 (Ref. 2).

5.0 CONCLUSIONS

The sting-vibration-compensation system substantially reduces the magnitude of oscillations which appear on force data traces as a result of sting vibrations. This permits more accurate force data to be taken from the traces since less curve fairing is required. It is especially useful in reducing data from runs of such a short duration that the period of oscillation of the data traces is greater than the length of the tunnel run, thus making accurate fairing of the curves impossible.

Although the compensation system removes the dynamic effects caused by the sting vibration, it does not compensate for forces produced by vibration of the model within itself. It becomes extremely difficult to fabricate some model configurations so that they are sufficiently rigid and yet light enough to permit their use without sting-vibration compensation. However, with the sting-vibration-compensation system, the model can be made heavier and stiffer to alleviate the difficulties which arise from model vibrations.

The optimum system is a compromise between the accuracy of the compensating system for increased model weights and the errors which arise from flexible models.

REFERENCES

1. Duryea, G. R., Martin, J. F., and Stevenson, L. M. "Instrumentation for Force and Pressure Measurements in a Hypersonic Shock Tunnel." Proceedings of the Second Symposium on Hypervelocity Techniques, Advances in Hypervelocity Techniques. University of Denver, March 1962.

2. Lukasiewicz, J., et al. ARS Preprint, # 1969-61, "Aerodynamic Testing at Mach Numbers from 15 to 20." Presented at International Hypersonics Conference, MIT, Cambridge, Mass., August 1961.

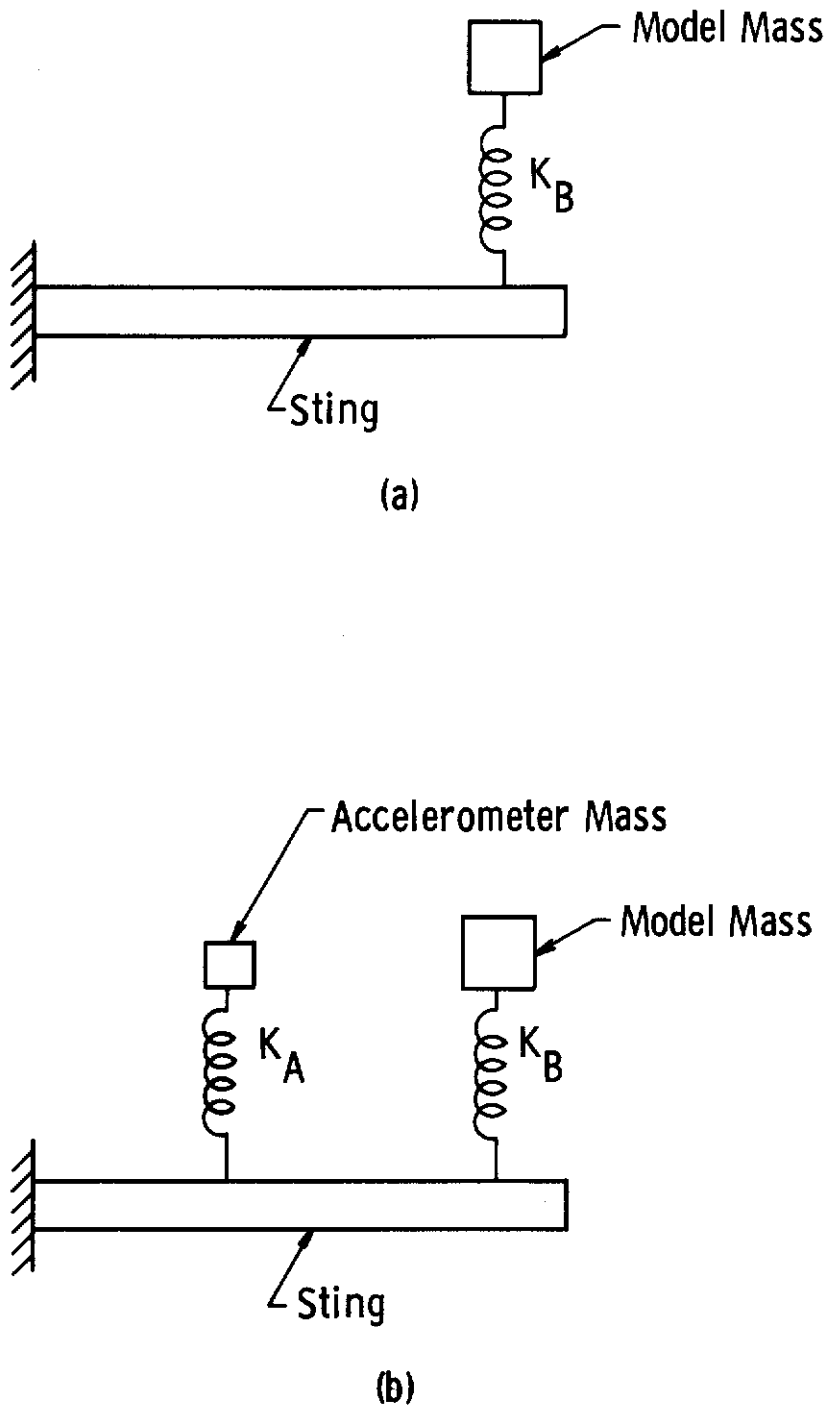

Fig. 1 Schematic Representation of Balance, Accelerometers, and Sting

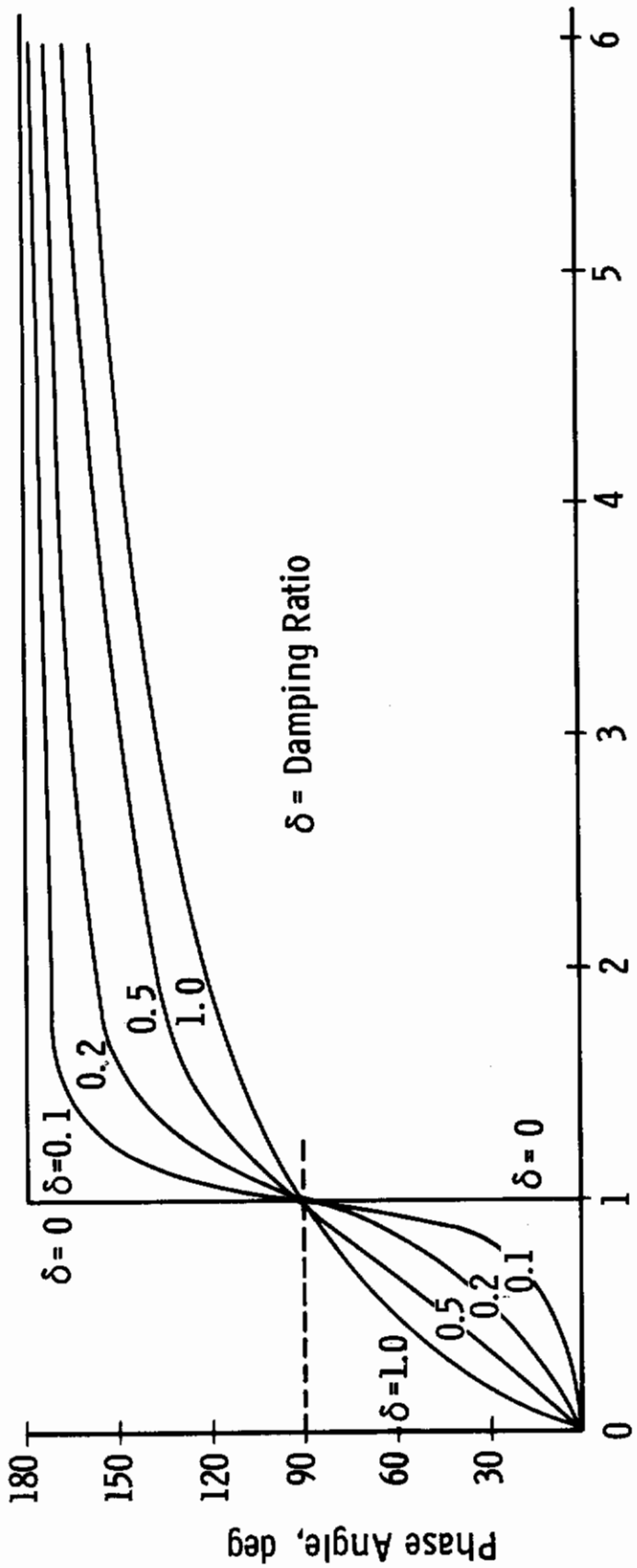

Fig. 2 Phase Angle between Forcing Function and Deflection for Different Values of Damping

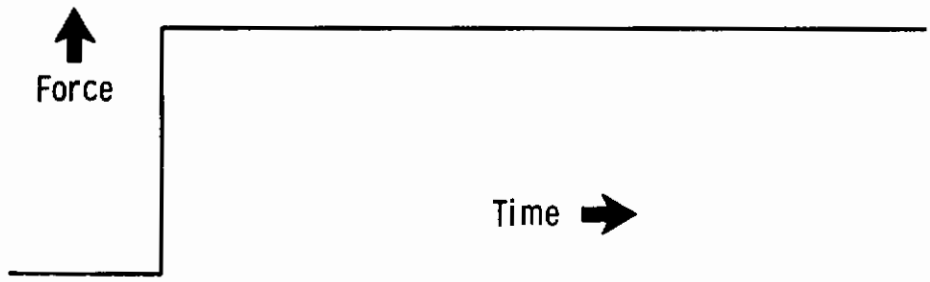

a. Forcing Function

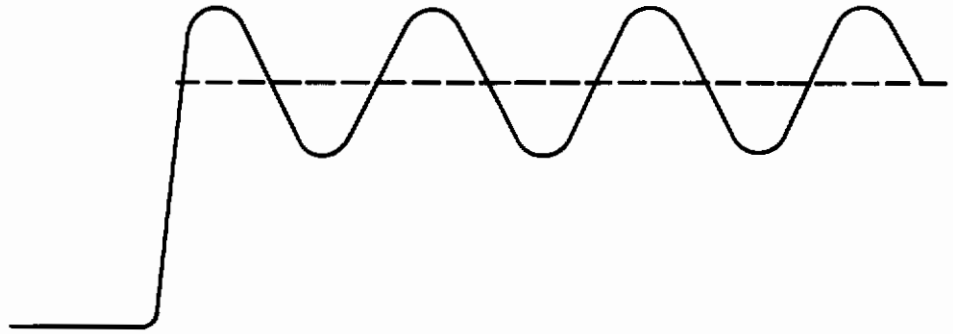

b. Balance Response to Forcing Function

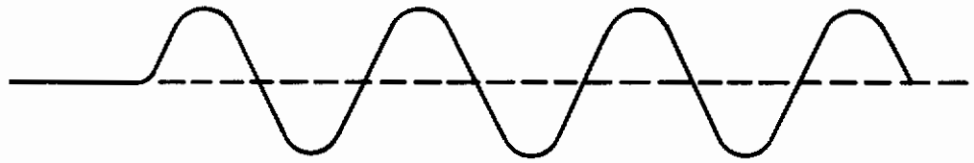

c. Accelerometer Response

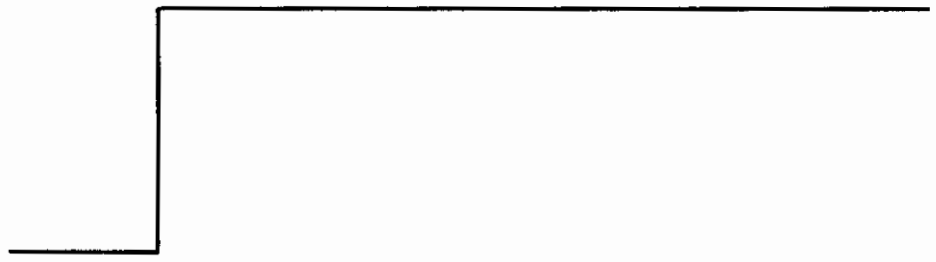

d. Sum of Balance and Accelerometer (accelerometer polarity reversed)

Fig. 3 Balance and Accelerometer Response to Step Force Input

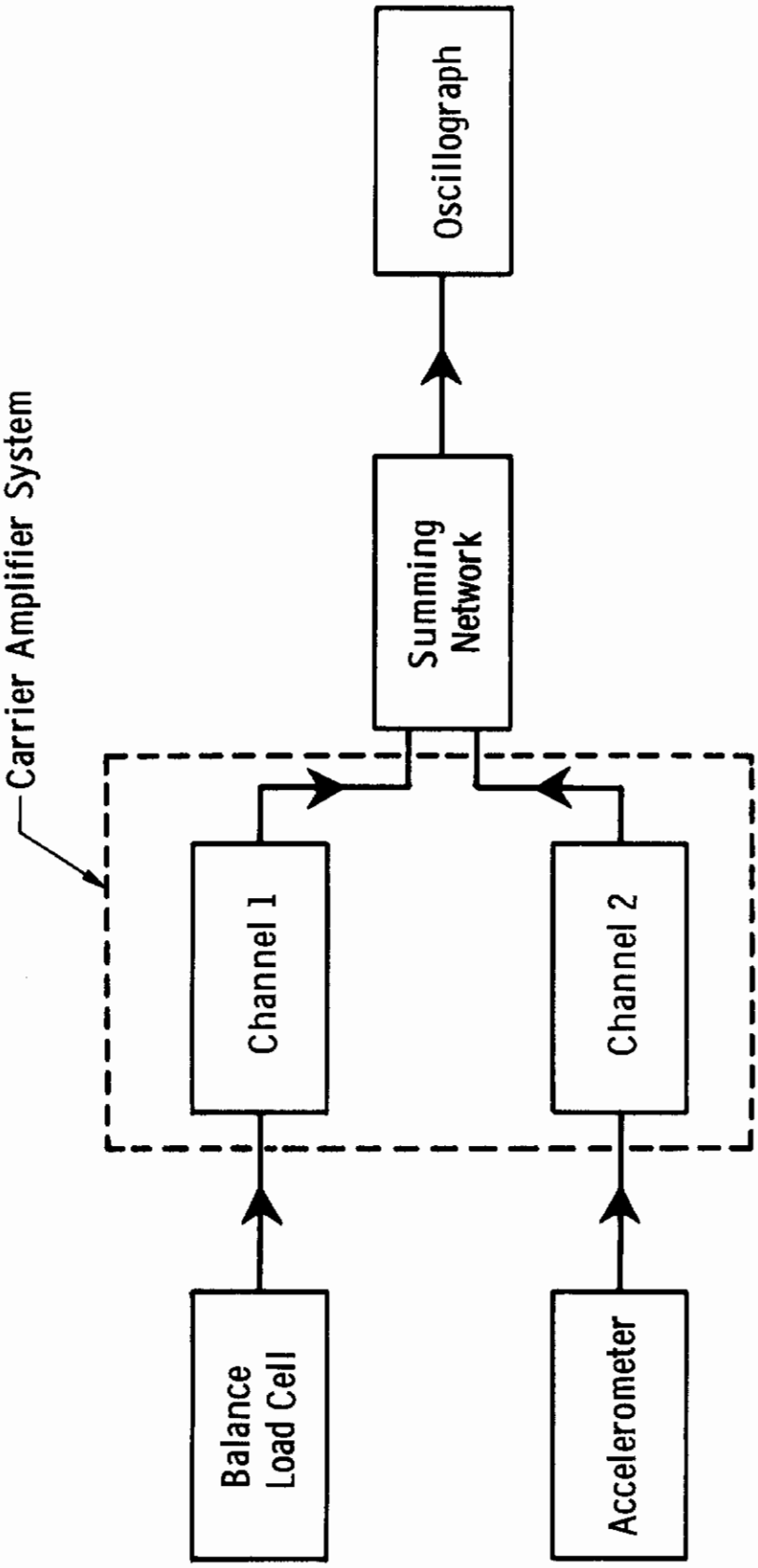

Fig. 4 Sting-Vibration-Compensation System

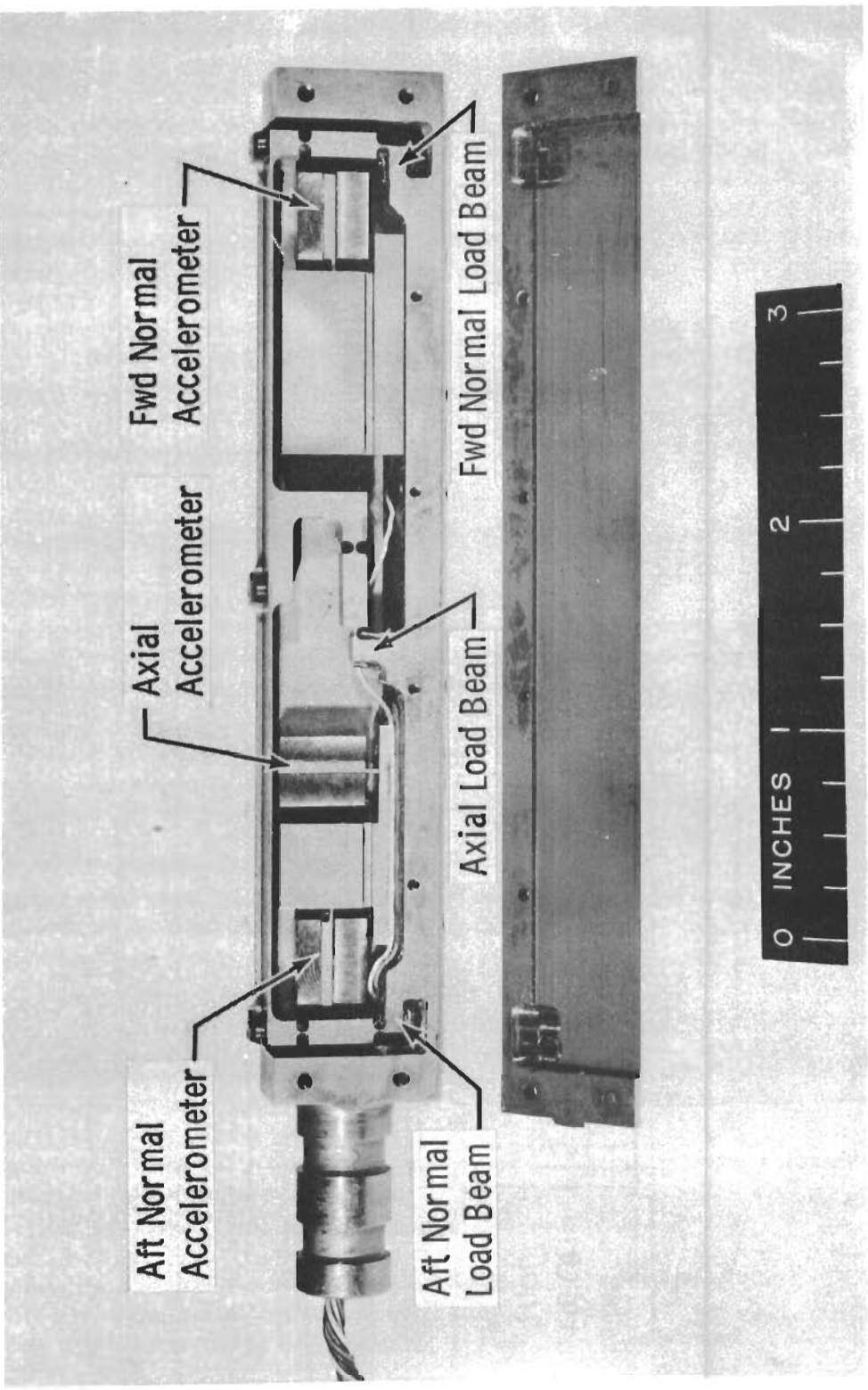

Fig. 5 Accelerometer-Instrumented Force Balance

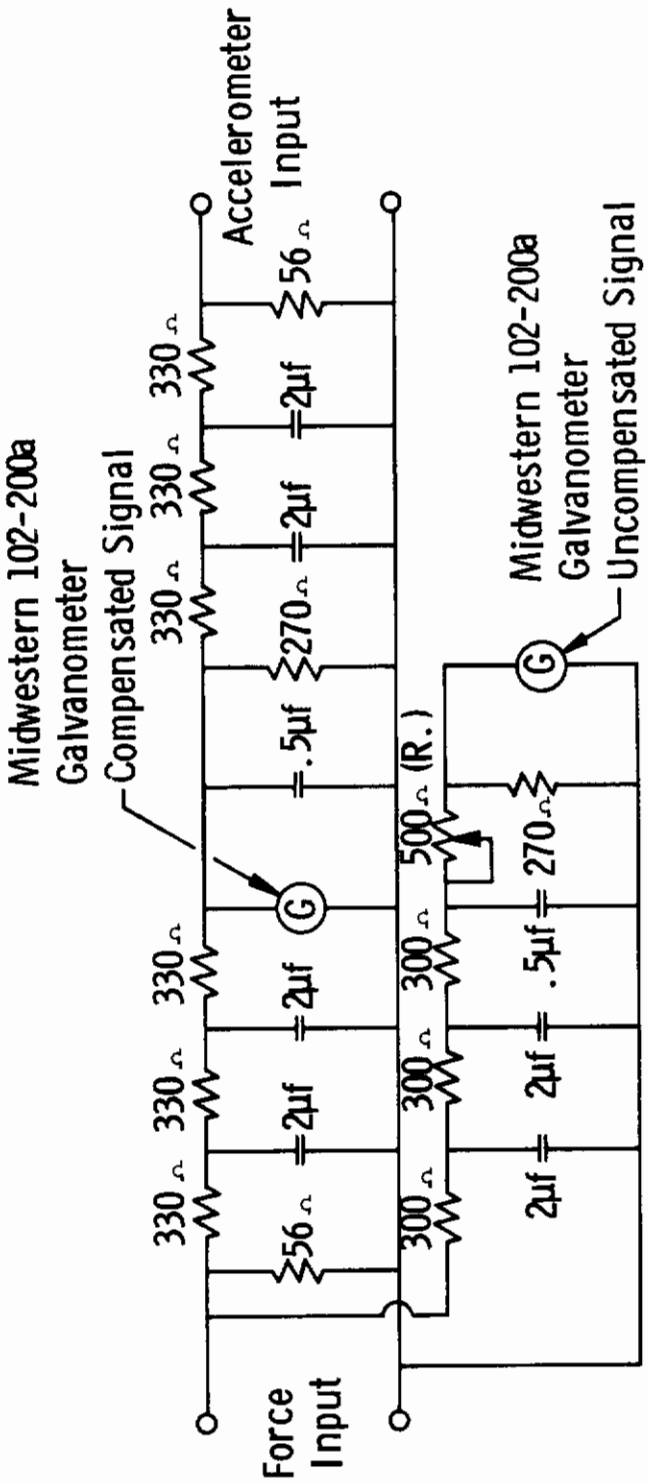

Fig. 6 Summing Network

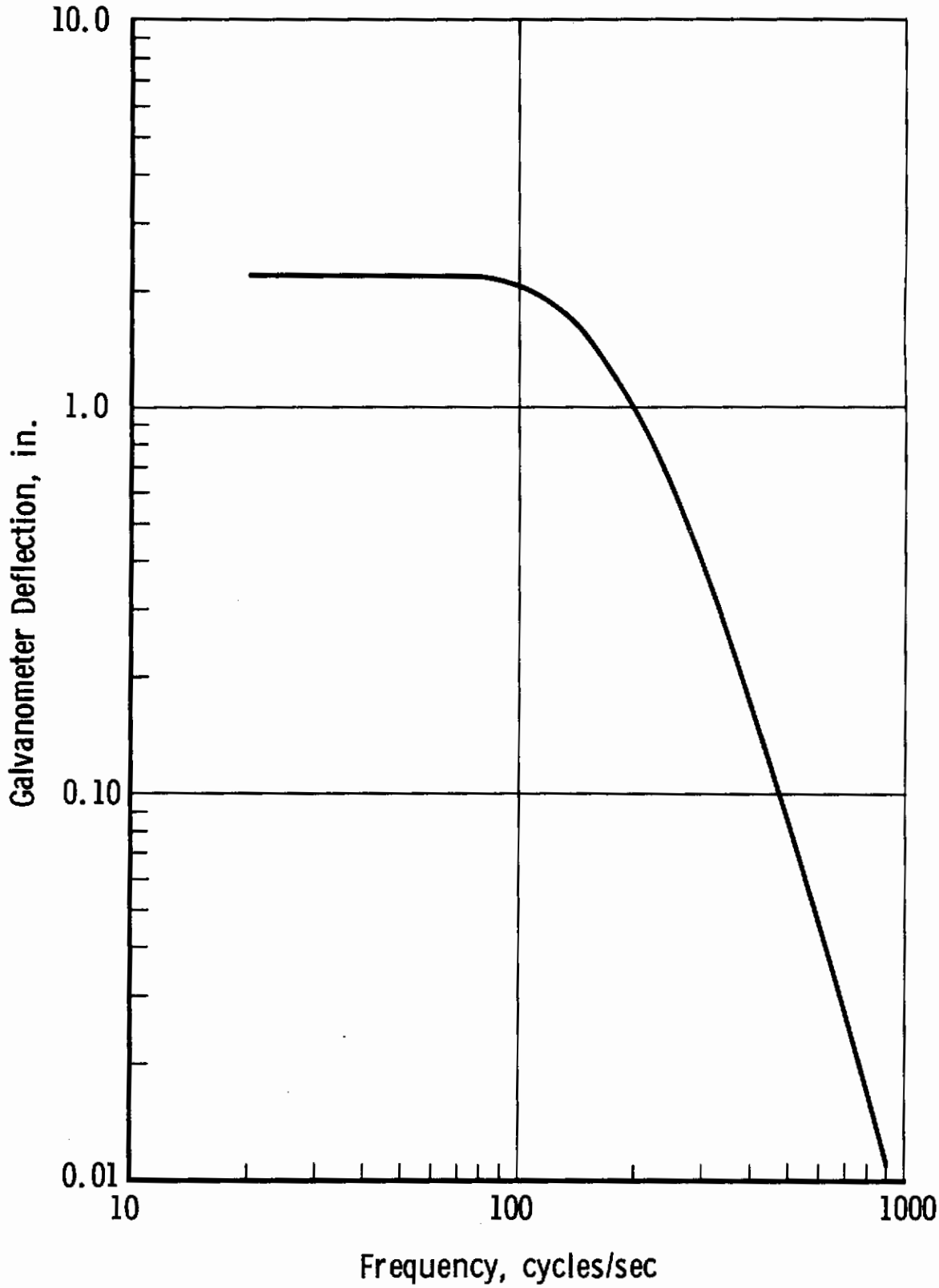

Fig. 7 Response Curve for Summing Network

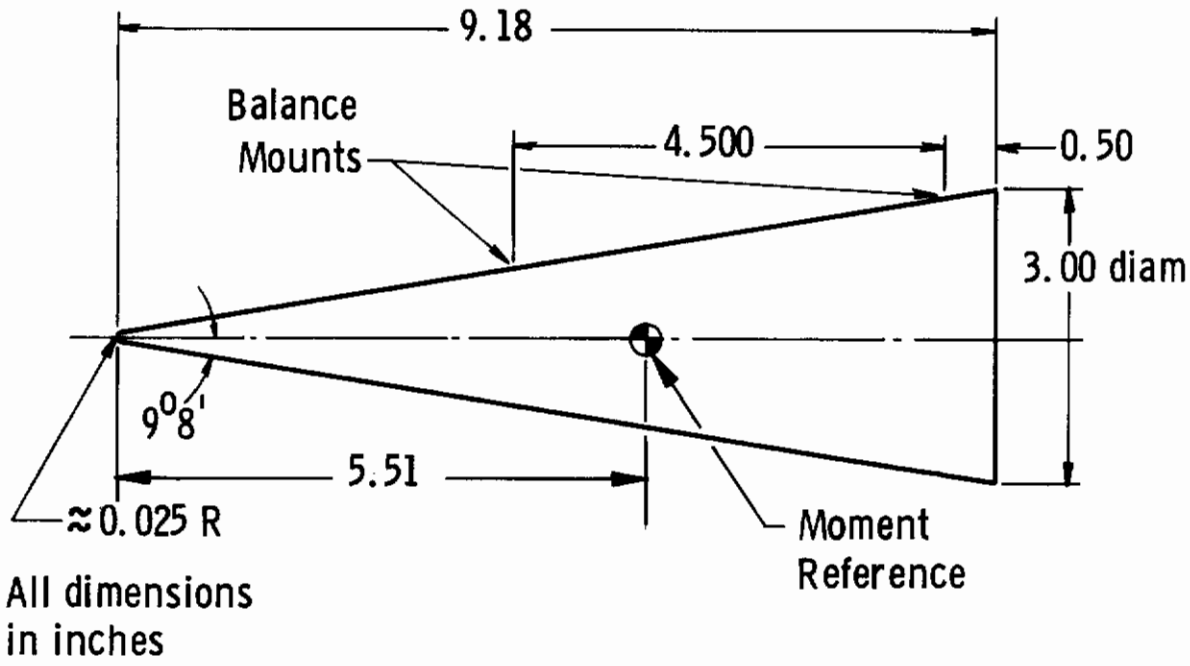

Fig. 8 Cone Model

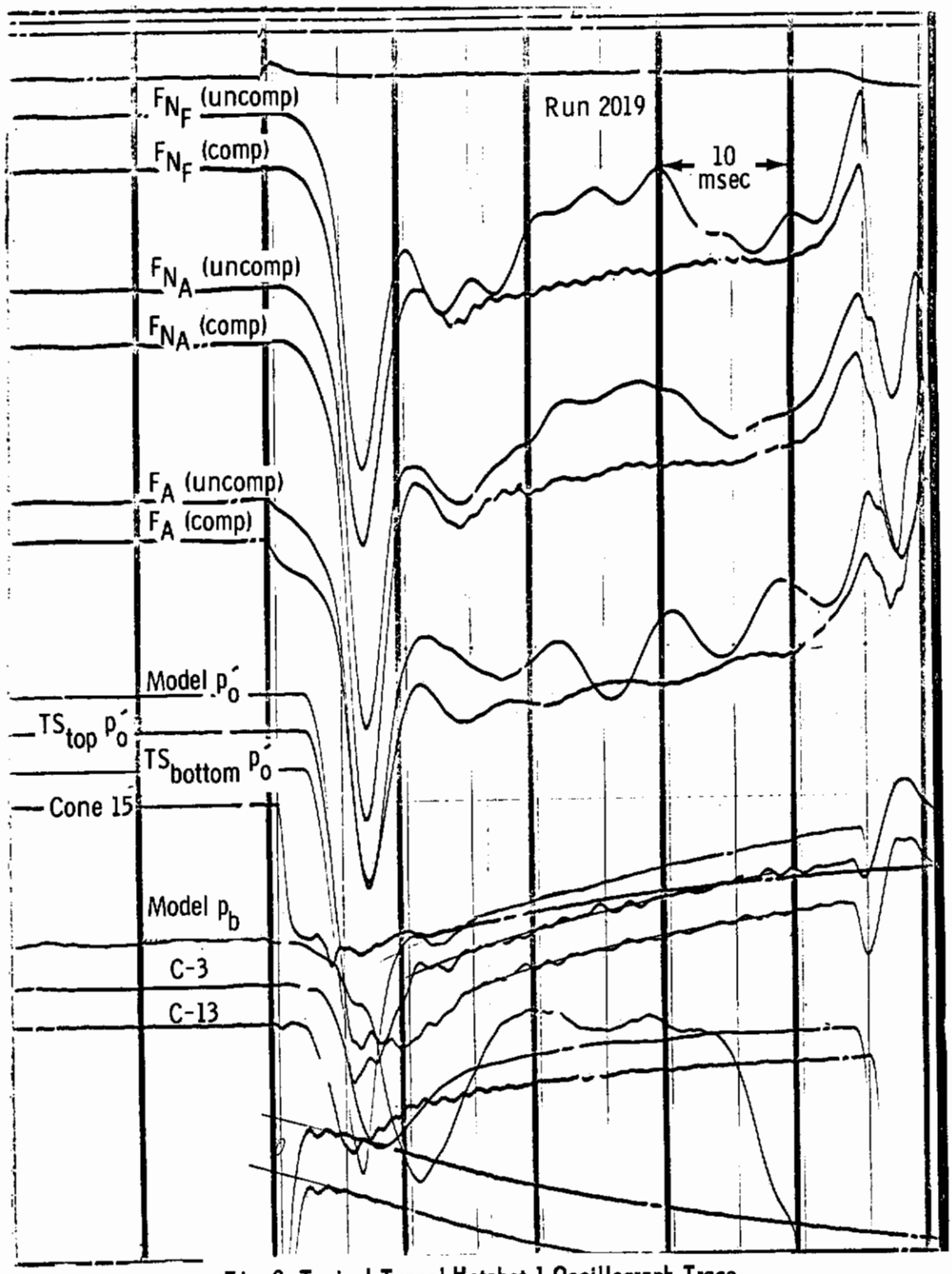

Fig. 9 Typical Tunnel Hotshot 1 Oscillograph Trace
(Model Mass = 52 gm, α = 10 deg)

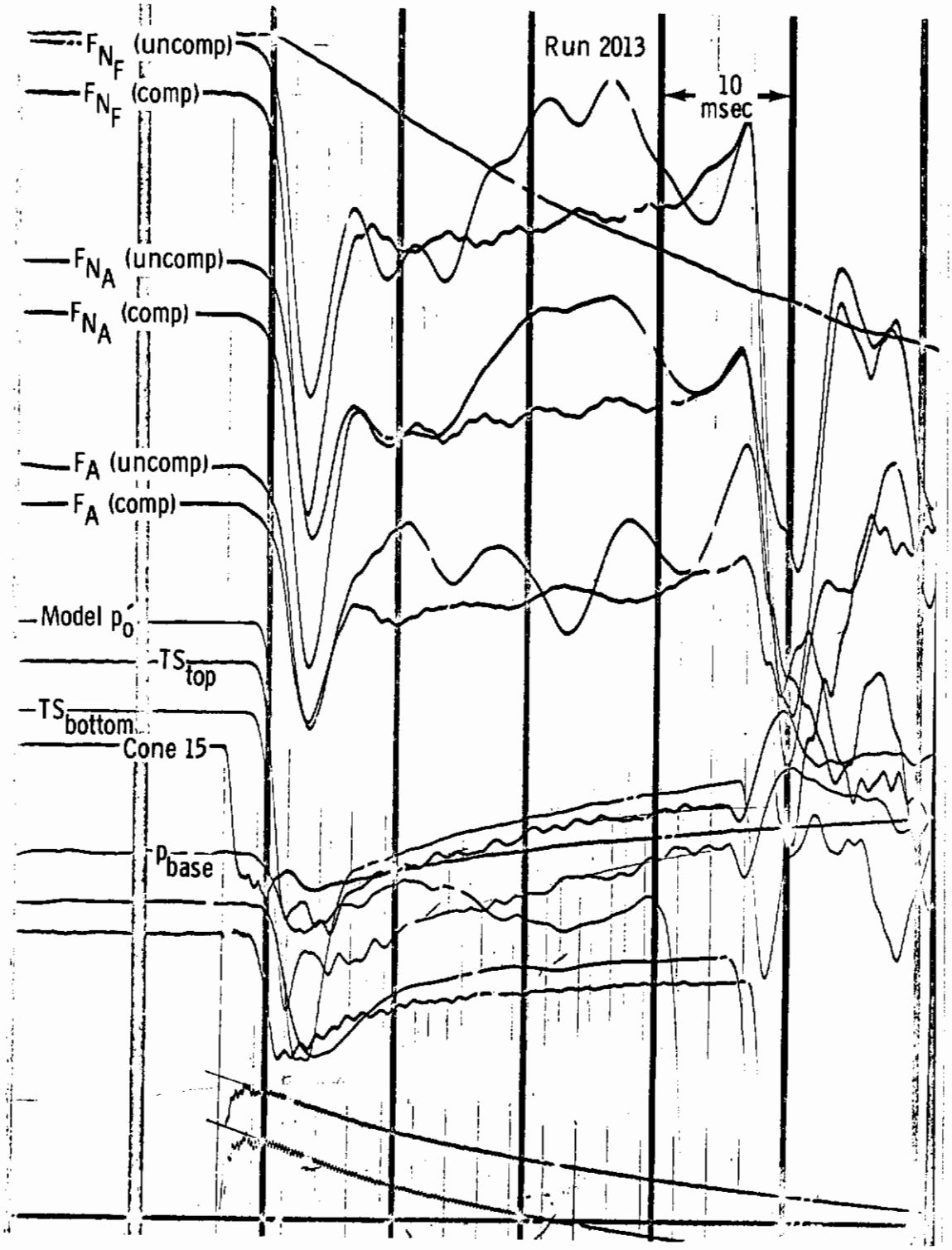

Fig. 10 Typical Tunnel Hotshot 1 Oscillograph Trace
(Model Mass = 144 gm, α = 15 deg)

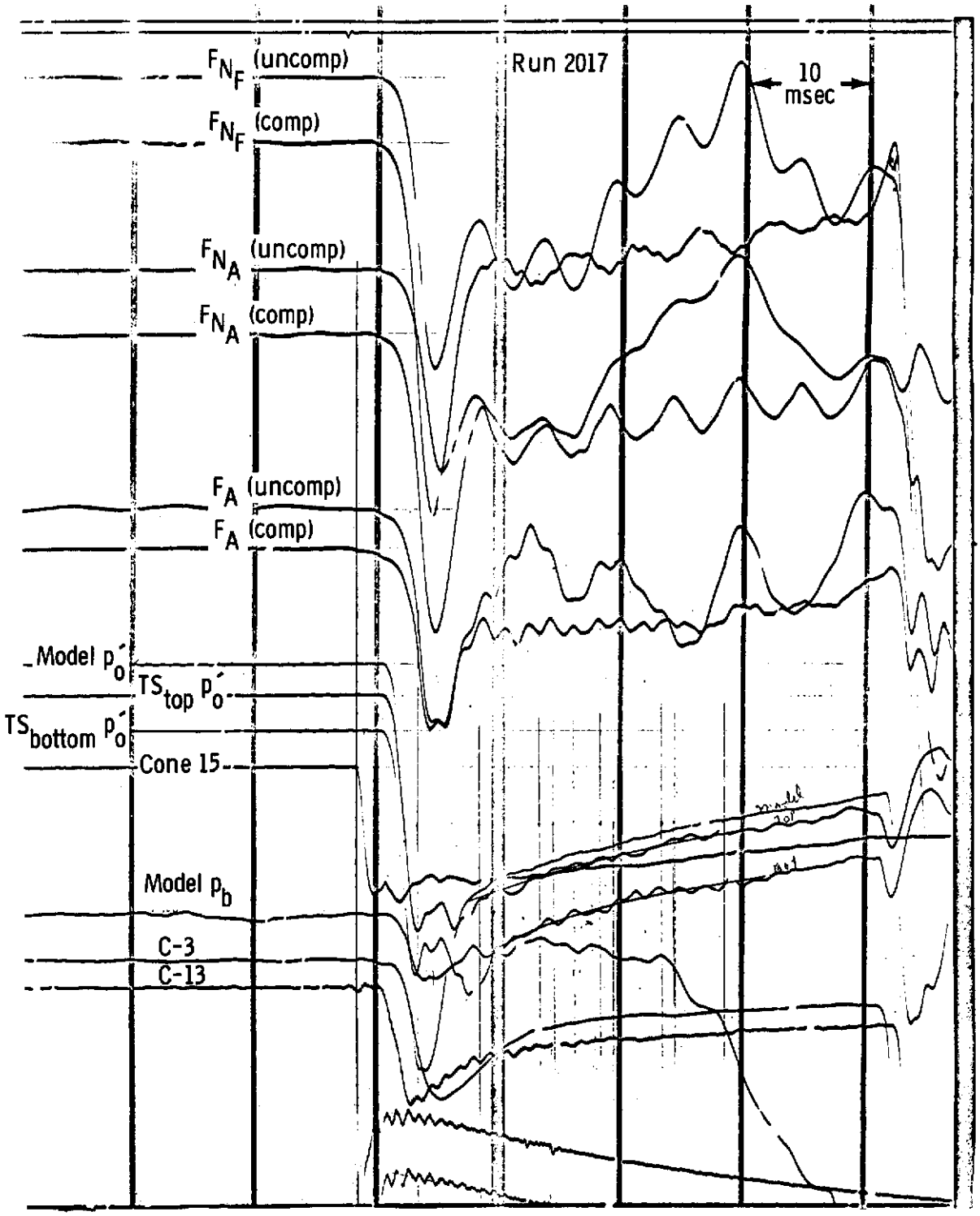

Fig. 11 Typical Tunnel Hotshot 1 Oscillograph Trace
(Model Mass = 237 gm, α = 15 deg)

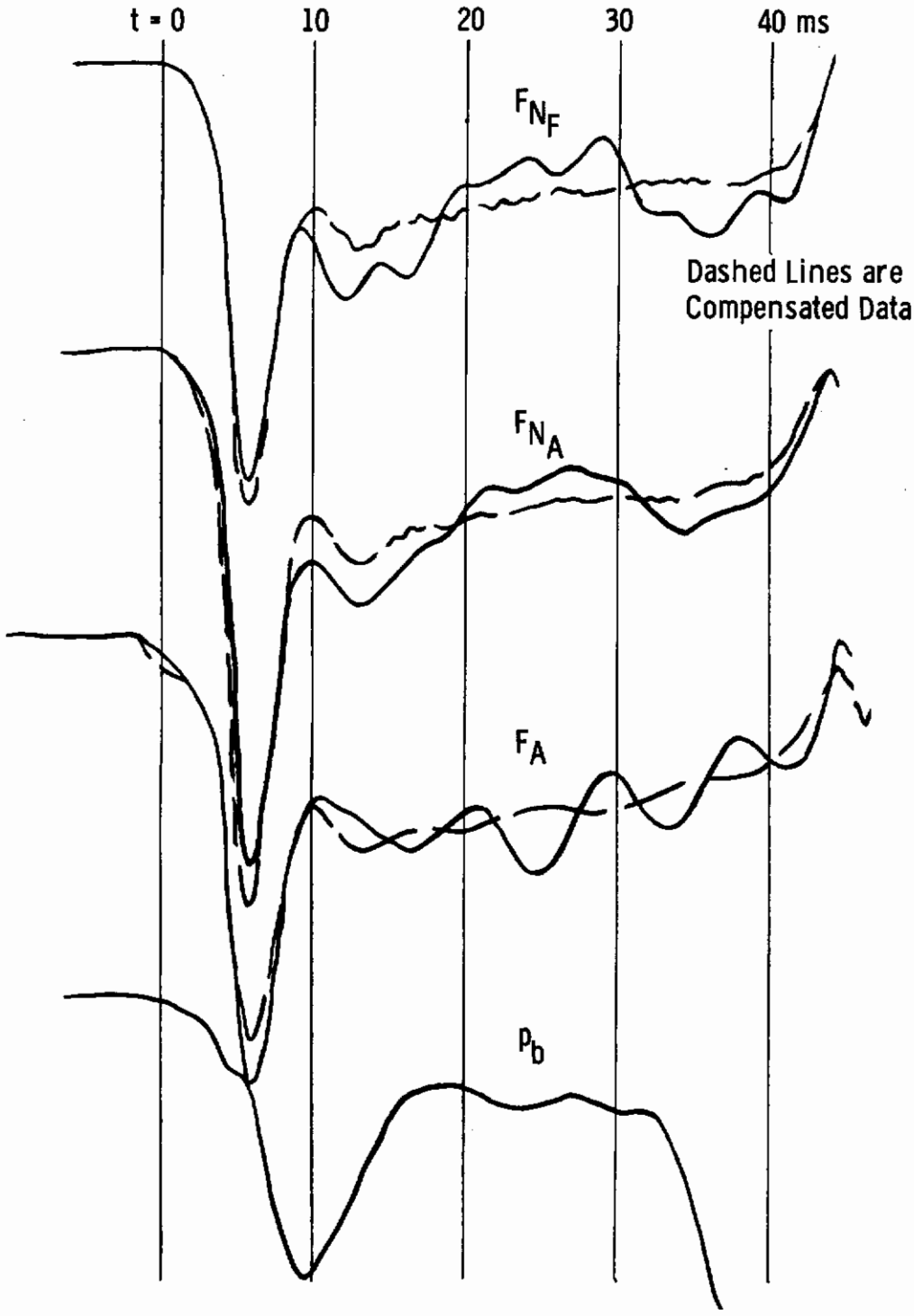

Fig. 12 Typical Oscillograph Trace with Zeros Displaced
(Model Mass = 52 gm, α = 10 deg)

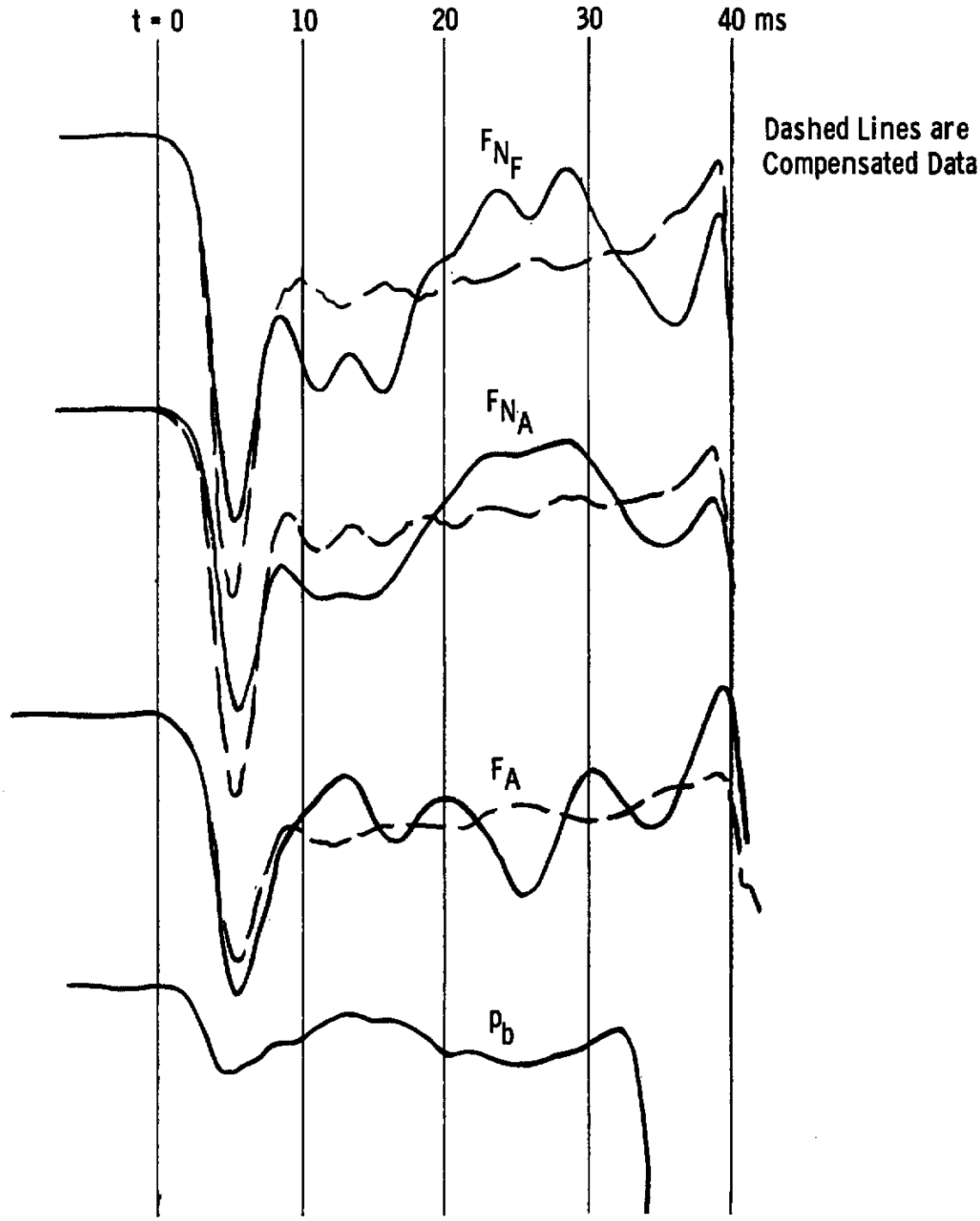

Fig. 13 Typical Oscillograph Trace with Zeros Displaced
(Model Mass = 144 gm, α = 15 deg)

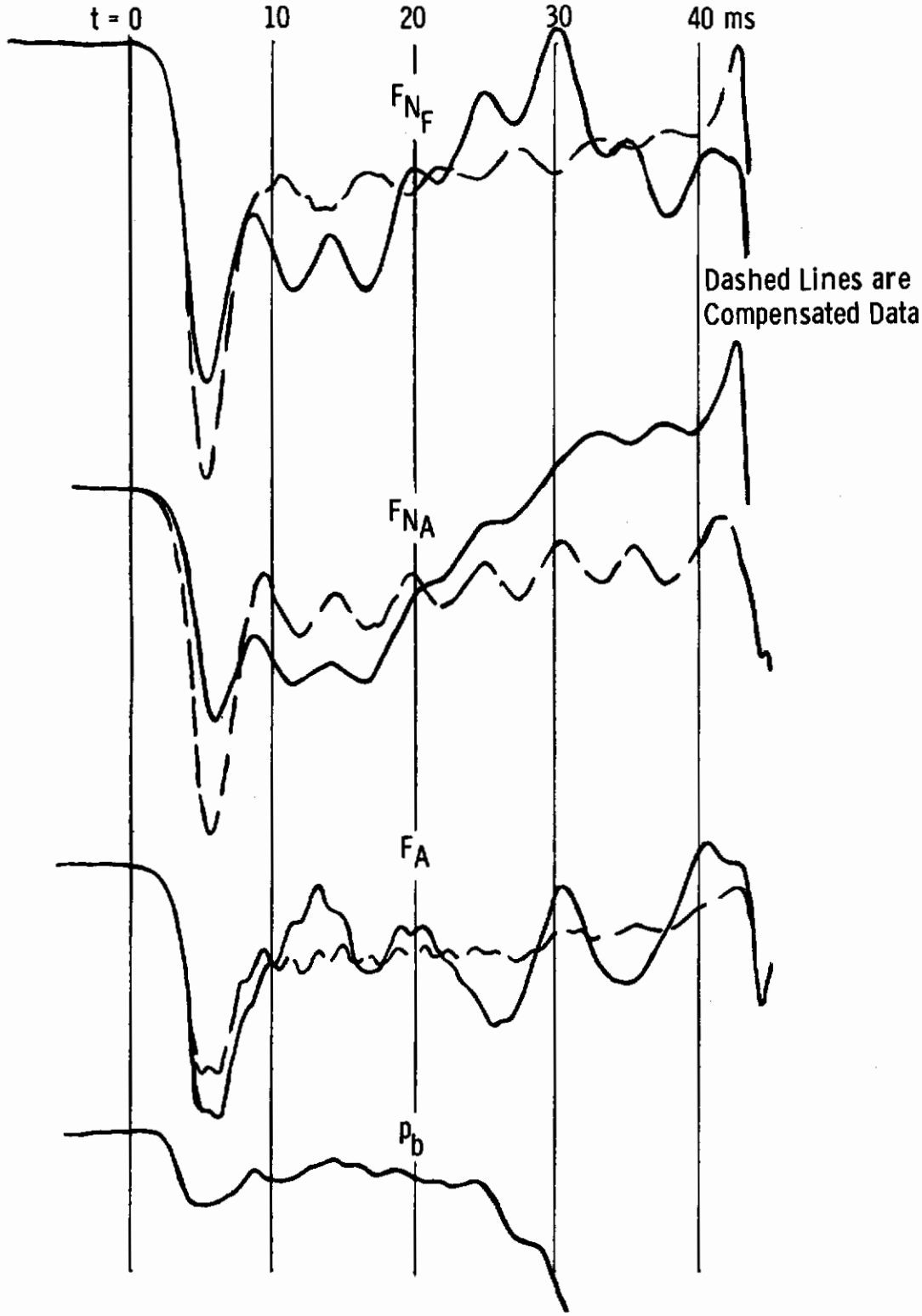

Fig. 14 Typical Oscillograph Trace with Zeros Displaced
(Model Mass = 237 gm, α = 15 deg)

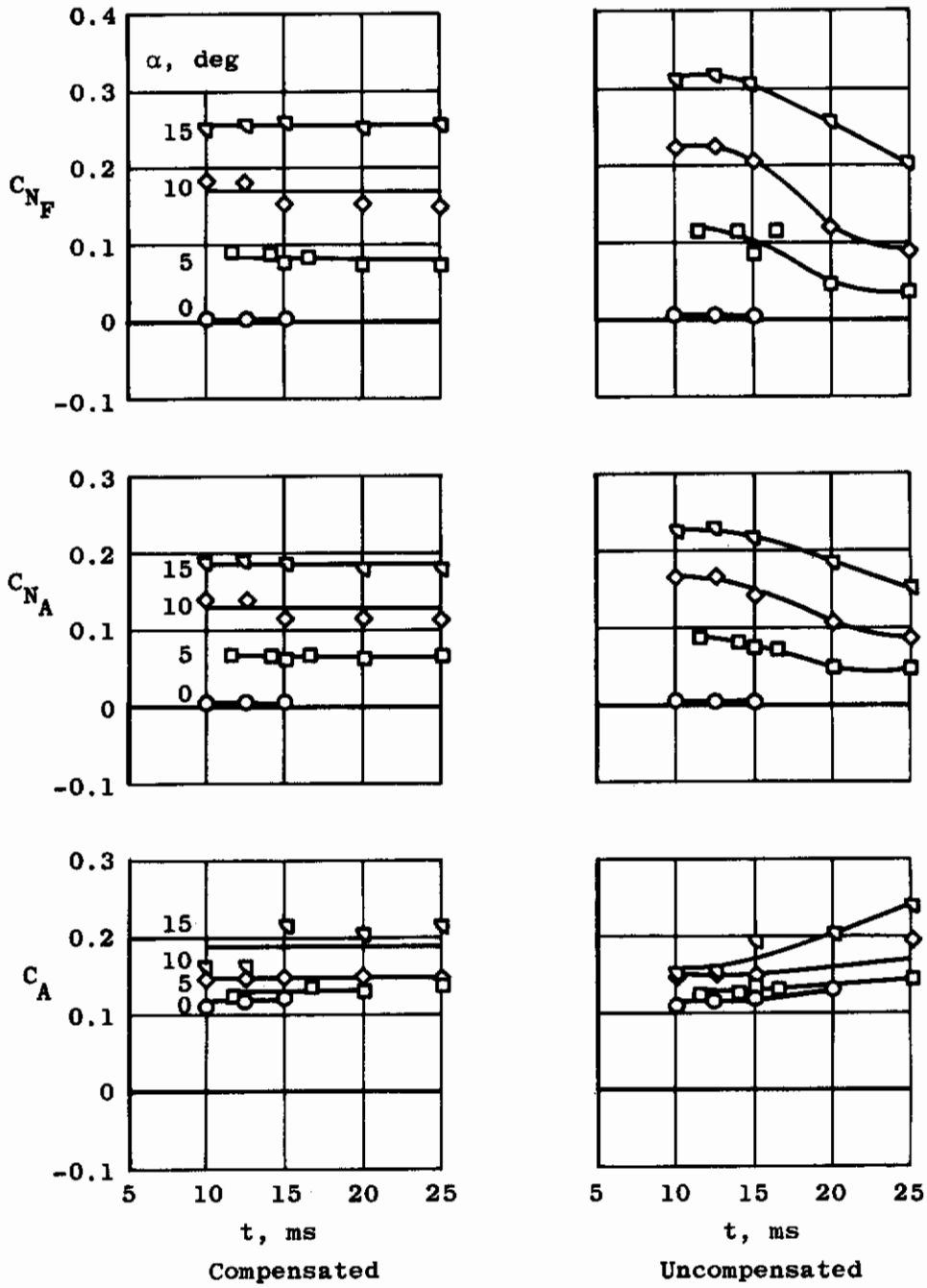

Fig. 15 Time Variation of Force Coefficients
(Model Weight = 52 gm)

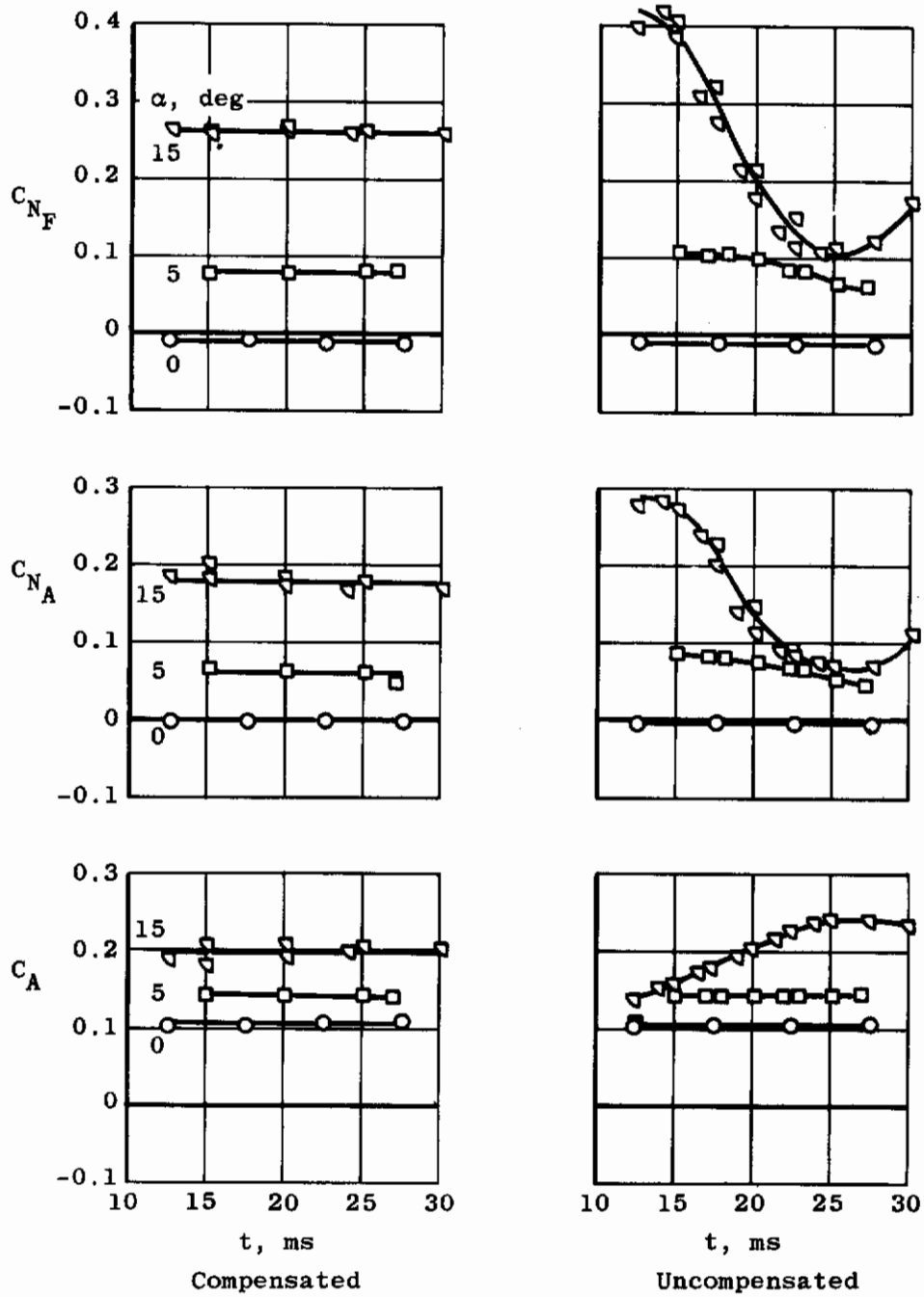

Fig. 16 Time Variation of Force Coefficients
(Model Weight = 144 gm)

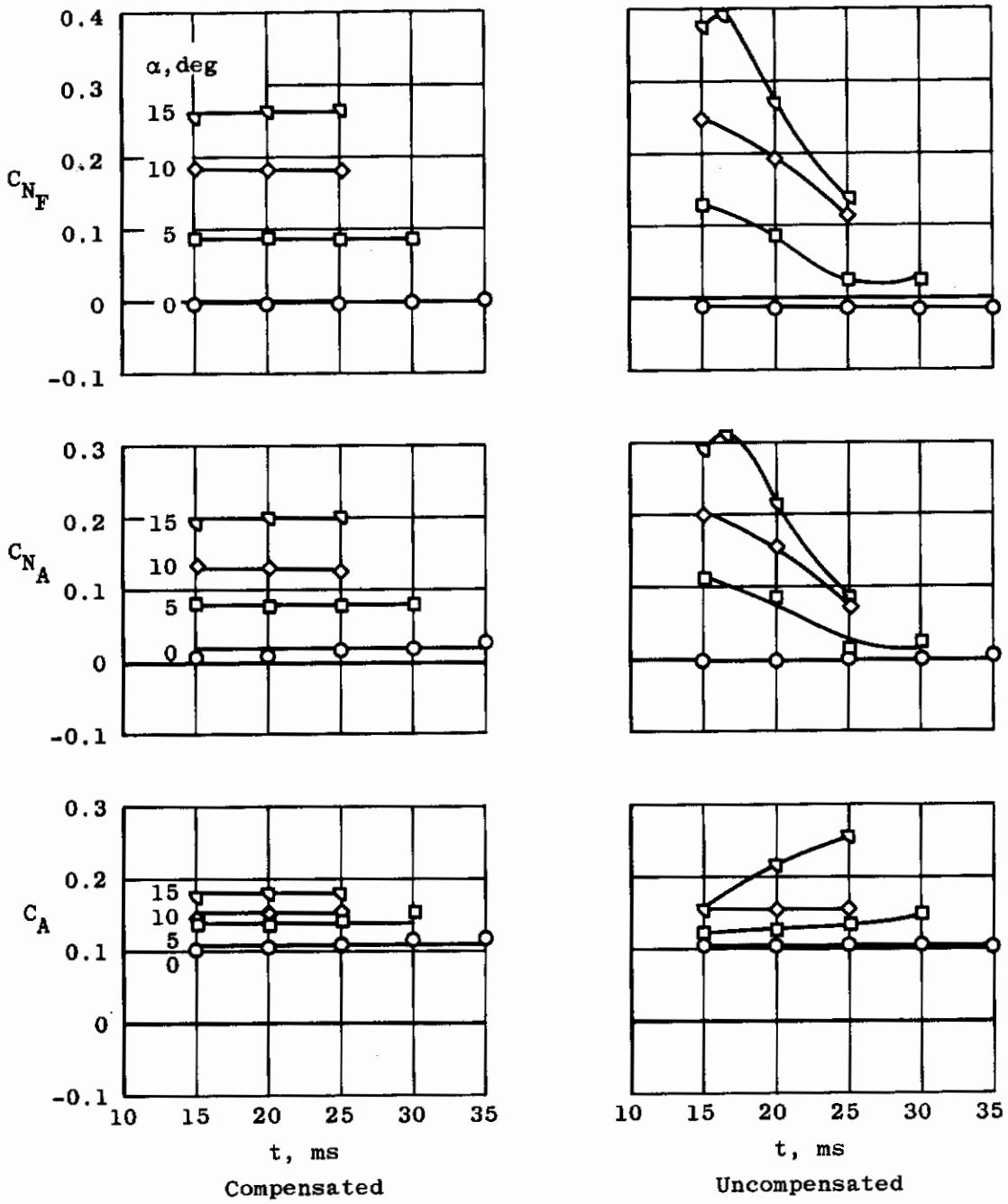

Fig. 17 Time Variation of Force Coefficients
(Model Weight = 237 gm)

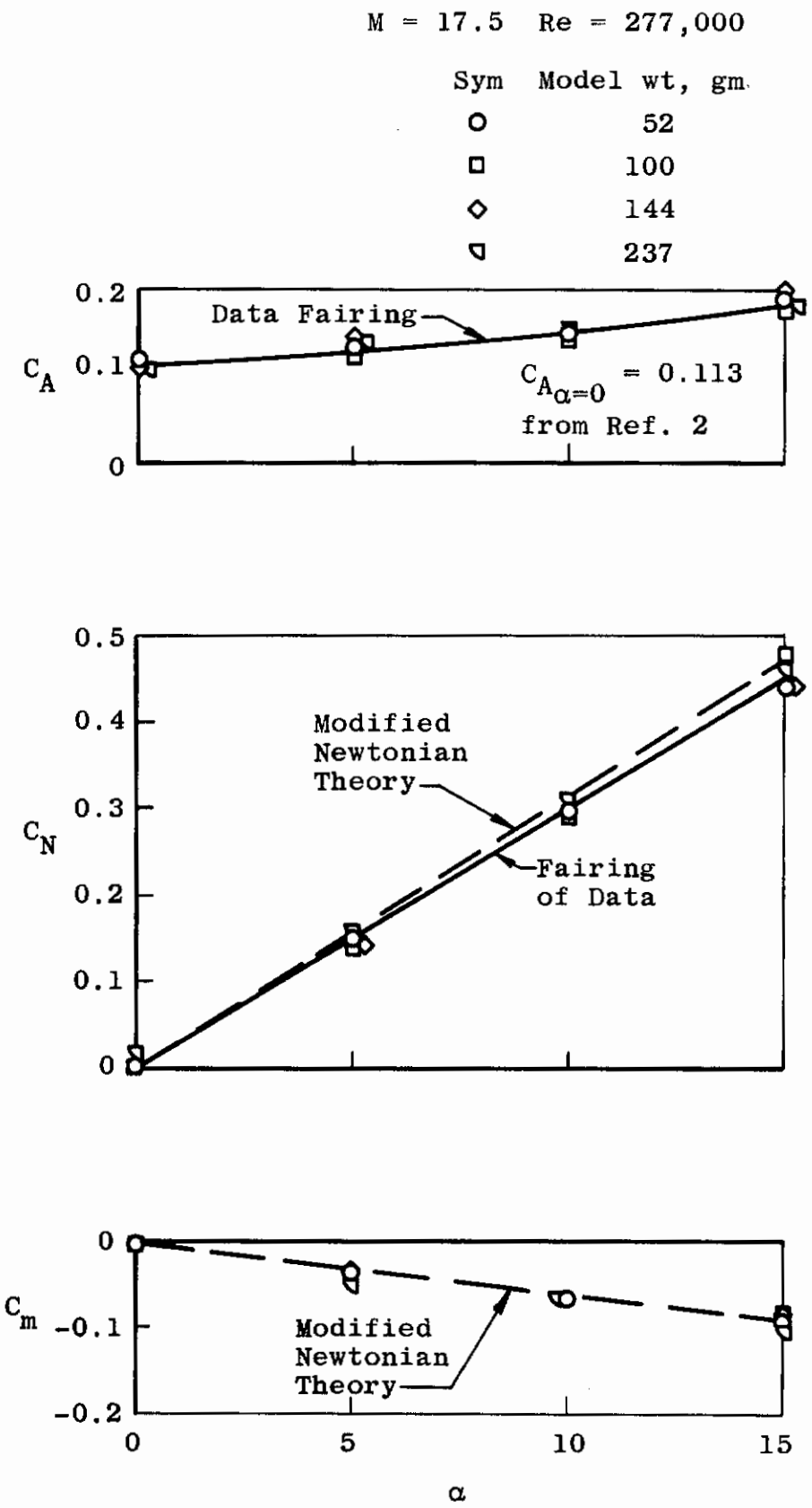

Fig. 18 Compensated Data versus Angle of Attack